JOURNAL OF BACTERIOLOGY, Sept. 2008, p. 5890–5897 Vol. 190, No. 17
0021-9193/08/$08.00+0 doi:10.1128/JB.00459-08

The Uncharacterized Transcription Factor YdhM Is the Regulator of the *nemA* Gene, Encoding *N*-Ethylmaleimide Reductase[▽]

Yoshimasa Umezawa, Tomohiro Shimada, Ayako Kori, Kayoko Yamada, and Akira Ishihama*

Department of Frontier Bioscience, Hosei University, Koganei, Tokyo 184-8584, Japan

Received 3 April 2008/Accepted 13 June 2008

***N*-Ethylmaleimide (NEM) has been used as a specific reagent of Cys modification in proteins and thus is toxic for cell growth. On the *Escherichia coli* genome, the *nemA* gene coding for NEM reductase is located downstream of the gene encoding an as-yet-uncharacterized transcription factor, YdhM. Disruption of the *ydhM* gene results in reduction of *nemA* expression even in the induced state, indicating that the two genes form a single operon. After in vitro genomic SELEX screening, one of the target recognition sequences for YdhM was identified within the promoter region for this *ydhM-nemA* operon. Both YdhM binding in vitro to the *ydhM* promoter region and transcription repression in vivo of the *ydhM-nemA* operon by YdhM were markedly reduced by the addition of NEM. Taken together, we propose that YdhM is the repressor for the *nemA* gene, thus hereafter designated NemR. The repressor function of NemR was inactivated by the addition of not only NEM but also other Cys modification reagents, implying that Cys modification of NemR renders it inactive. This is an addition to the mode of controlling activity of transcription factors by alkylation with chemical agents.**

N-Ethylmaleimide (NEM) with a specific activity of Cys modification has been widely used for the molecular dissection of proteins. Since Cys is often located within the catalytic domain of enzymes, NEM treatment renders this group of enzymes inactive. For instance, NEM treatment of RNA polymerase (6) and the sigma subunit (13) of *Escherichia coli* results in inactivation of the catalytic activity of RNA polymerization and the promoter recognition activity, respectively. *E. coli* ribosomes are also inactivated by treatment with NEM (11, 24). Accordingly NEM is a toxic compound for cell growth.

Using the gene mapping membrane technique, Miura et al. (10) identified a gene (*nemA*) that encodes NEM reductase in *E. coli*. The *nemA* gene encodes a polypeptide of 365 amino acids with a molecular mass of 39,514 Da. NemA is also involved in reductive degradation of other toxic nitrous compounds besides NEM. For instance, some *E. coli* laboratory strains have multiple enzymes that degrade 2,4,6-trinitrotoluene (TNT) for release of nitrite from the nitroaromatic ring, yielding 2-hydroxylamino-6-nitrotoluene (5). In addition to NemA, both NfsA and NfsB nitroreductases catalyze TNT reduction, converting the nitro groups on the aromatic ring to the corresponding hydroxylamino derivatives (1, 17, 29). All these nitroreductases degrade toxic nitrous compounds, ultimately releasing ammonium ions that can, in turn, be used as a nitrogen source by *E. coli* for growth. In spite of a growing interest in the removal and degradation of toxic nitrous compounds from polluted environments, our current knowledge of the roles and regulation of corresponding nitroreductases is limited, and in particular, little is known of the regulation of synthesis of these enzymes.

Upstream of the *nemA* gene, a putative gene encoding an as-yet-uncharacterized transcription factor, YdhM, is located. For a systematic search for target genes and promoters recognized by approximately 300 species of DNA-binding transcription factors in *E. coli*, we developed the genomic SELEX system, in which transcription factor-associated DNA sequences can be isolated from mixtures of genome DNA fragments (19). After sequence analysis of the transcription factor-associated sequences, the target genes and promoters can be identified. Using this newly developed genomic SELEX system, screening of target genes and promoters has been performed for the putative transcription factor YdhM. Taking all results herein described, we propose that YdhM is the regulator for the *nemA* transcription unit and should be renamed NemR. One unique feature of NemR is that the repressor function of NemR is inactivated after protein alkylation by inducers. The mode of activity control by NemR repressor is thus similar to that of Ada protein, which repairs DNA methyl phosphotriester lesions by transferring the methyl group to its Cys residue, thereby acting as a positive regulator for its own synthesis as well as other DNA alkylation response genes (12).

MATERIALS AND METHODS

Bacterial strains. *Escherichia coli* KP7600 (W3110 *lacI*^{q} *lacZ*ΔM15 *galK2 galT22*) and JD22799 (transposon insertion at position +130 within the *nemR* coding sequence of KP7600 in opposite direction from *nemR*; a gift from T. Miki, Fukuoka Dental College) were used in various experiments for analysis of the regulatory roles of NemR, including primer extension assay, Northern blot analysis, and promoter assay. *E. coli* BL21(DE3) [F^- *ompT hsd*(r_B^- m_B^-) *dcm gal* λ(DE3)] was used for expression and purification of NemR. Cells were cultured in LB medium or M9-0.4% glucose medium at 37°C. When necessary, 100 μg/ml ampicillin was added to the medium.

Expression and purification of His-tagged NemR protein. For construction of plasmid pNemR for NemR expression, a DNA fragment corresponding to the NemR coding sequence was amplified by PCR using *E. coli* W3110 genome DNA as a template and a pair of primers which were designed so as to hybridize upstream or downstream of the NemR coding sequence. After digestion with NdeI and NotI (note that the restriction enzyme sites were included within the primer sequences), PCR products were cloned into pET21a(+) (Novagen) between NdeI and NotI sites. The plasmid construct was confirmed by DNA sequencing. For protein expression, pNemR plasmid was transformed into *E. coli* BL21(DE3). Transformants were grown in 200 ml of LB medium, and at a cell

* Corresponding author. Mailing address: Department of Frontier Bioscience, Hosei University, Koganei, Tokyo 184-8584, Japan. Phone and fax: 81-42-387-6231. E-mail: aishiham@hosei.ac.jp.

▽ Published ahead of print on 20 June 2008.

density of 0.6 at 600 nm, IPTG (isopropyl-β-D-thiogalactopyranoside) was added at a final concentration of 1 mM. After 3 h of incubation, cells were harvested by centrifugation, washed with a lysis buffer (50 mM Tris-HCl, pH 8.0 at 4°C, 100 mM NaCl), and then stored at −80°C until use.

For protein purification, frozen cells were suspended in 3 ml of lysis buffer containing 100 mM phenylmethylsulfonyl fluoride. Cells were treated with lysozyme and then subjected to sonication for cell disruption. After centrifugation at 15,000 rpm for 20 min at 4°C, the resulting supernatant was mixed with 2 ml of 50% nickel-nitrilotriacetic acid agarose solution (Qiagen) and loaded onto a column. After being washed with 10 ml of the lysis buffer, the column was washed with 10 ml of washing buffer (50 mM Tris-HCl, pH 8.0 at 4°C, 100 mM NaCl) and then 10 ml of washing buffer containing 10 mM imidazole. Proteins were eluted with 2 ml of an elution buffer (lysis buffer plus 200 mM imidazole), and NemR peak fractions were pooled and dialyzed against a storage buffer (50 mM Tris-HCl, pH 7.6 at 4°C, 200 mM KCl, 10 mM $MgCl_2$, 0.1 mM EDTA, 1 mM dithiothreitol, and 50% glycerol) and stored at −80°C until use. Protein purity was checked by sodium dodecyl sulfate-polyacrylamide gel electrophoresis (PAGE).

SELEX search for NemR-binding sequences. The genomic SELEX system was used as described previously (19). Genome DNA of *E. coli* W3110 was sonicated to generate fragments of 150 to 300 bp in length. The *E. coli* DNA library was constructed after cloning of these 150- to 300-bp DNA fragments into plasmid pBR322 at the EcoRV site. A collection of 150- to 300-bp DNA fragments could be regenerated by PCR amplification using the *E. coli* DNA plasmid library as the template and a set of primers, EcoRV-F (5′-CTTGGTTATGCCGGTACT GC-3′) and EcoRV-R (5′-GCGATGCTGTCGGAATGGAC-3′), which hybridize to pBR322 vector at EcoRV junctions. PCR products thus generated were purified by 5% PAGE. For the genomic SELEX screening of NemR-binding sequences, 5 pmol of DNA fragments and 20 pmol of His-tagged NemR were mixed in a binding buffer (10 mM Tris-HCl, pH 7.8 at 4°C, 3 mM magnesium acetate, 150 mM NaCl, 1.25 μg/ml bovine serum albumin) and incubated for 30 min at 37°C. The mixture was applied onto a nickel-nitrilotriacetic acid column, and after unbound DNA was washed with the binding buffer containing 10 mM imidazole, DNA-NemR complexes were eluted with an elution buffer containing 200 mM imidazole. When necessary, this SELEX cycle was repeated several times. For sequencing of NemR-bound DNA fragments, DNA was isolated from DNA-NemR complexes by PAGE and PCR amplified. PCR products were cloned into pT7 Blue-T vector (Novagen) using the blunt-end cloning kit (Takara) and transformed into *E. coli* DH5α. Sequencing analysis was carried out using T7 primer (5′-TAATACGACTCACTATAGGG-3′) with an ABI 3130xl DNA sequencer.

Gel mobility shift assay. The gel shift assay was performed as described previously (14, 15). In brief, probes were generated by PCR amplification of NemR-binding sequences in SELEX using a pair of primers, 5′-fluorescein isothiocyanate (FITC)-labeled T7-F primer (5′-TAATACGACTACTATAGG G-3′) and T7-R primer (5′-GGTTTTCCCAGTCACACGACG-3′); the genomic SELEX plasmids containing the respective NemR recognition sequences as templates; and Ex *Taq* DNA polymerase (Takara). PCR products with FITC at their termini were purified by PAGE. For gel shift assays, 0.3 pmol each of the FITC-labeled probes was incubated at 37°C for 30 min with various amounts of NemR in 12 μl of gel shift buffer consisting of 10 mM Tris-HCl, pH 7.8 at 4°C, 150 mM NaCl, and 3 mM magnesium acetate. After addition of a DNA dye solution, the mixture was directly subjected to 6% PAGE. Fluorescence-labeled DNA in gels was detected using the Pharos FX Plus system (Bio-Rad).

DNase I footprinting assay. The DNase I footprinting assay was carried out using FITC-labeled DNA fragments as described previously (15, 16). Each 0.5 pmol of FITC-labeled probes was incubated at 37°C for 30 min with various amounts of NemR in DNase I footprinting buffer consisting of 25 μl of 10 mM Tris-HCl (pH 7.8), 150 mM NaCl, 3 mM magnesium acetate, 5 mM $CaCl_2$, and 25 μg/ml bovine serum albumin. After incubation for 30 min, DNA digestion was initiated by the addition of 5 ng of DNase I (Takara). After digestion for 30 s at 25°C, the reaction was terminated by the addition of 25 μl of phenol. Digested products were precipitated with ethanol, dissolved in formamide-dye solution, and analyzed by electrophoresis on a 6% polyacrylamide gel containing 7 M urea.

Measurement of the promoter activity. Promoter strength was determined as described previously (9, 22). In brief, green fluorescent protein (GFP) was expressed under the control of a test promoter while red fluorescent protein (RFP) was under the control of a reference promoter. The promoter assay vector pGRP carries two types of fluorescent protein genes, one for RFP under the control of reference promoter *lacUV5* and the other for GFP under the control of a test promoter. The sequences upstream from the initiation codons of *ydhF*, *ydhL*, and *nemR* were PCR amplified using the respective primers and inserted into pGRP vector. These primers contain the sequences for recognition by EcoT22I, BglII, or BamHI, which can be used for promoter cloning. The PCR products were digested with the respective restriction enzymes and then ligated into pGRP at EcoT22I and BglII sites. The insertions in the promoter assay plasmids thus constructed were confirmed by sequencing, and the plasmids were named pGRP*ydhF*, pGRP*ydhL*, and pGRP*nemR*, respectively.

For the measurement of the fluorescence intensity of RFP or GFP expressed in *E. coli*, transformants, each carrying one promoter assay vector, were grown in LB medium or M9-0.4% glucose medium up to an optical density at 600 nm (OD_{600}) of 0.3 to 4.0, harvested by centrifugation, and resuspended in phosphate-buffered saline (−). The cell suspensions were diluted with phosphate-buffered saline (−) to obtain approximately the same cell density (OD_{600} of 0.6) for all samples. For the measurement of bulk fluorescence, aliquots of an 0.2-ml cell suspension were added to 0.4-ml flat-bottomed 96-well plates, and the fluorescence was measured with a Wallac 1420 ARVOsx counter (Perkin-Elmer Life Sciences), where GFP was measured using 485-nm excitation and 535-nm emission and RFP was measured using 544-nm excitation and 590-nm emission. The fluorescence intensity of GFP with the test promoter was normalized using the equation $(X/Y)/(A/B)$, in which X and Y indicate the fluorescence intensities of GFP (test promoter) and RFP (*lacUV5* promoter), respectively, while A and B represent the fluorescence intensities of GFP (*lacUV5* promoter) and RFP (*lacUV5* promoter), respectively.

Primer extension analysis. For preparation of total RNA for the primer extension analysis, overnight cultures of *E. coli* wild-type KP7600 and *nemR*-disrupted mutant JD22799, both carrying a promoter assay vector, pGRH045 (or pGRP*nemR*), were diluted 100-fold in 15 ml of LB medium and cells were grown to an OD_{600} of 3.2 (late stationary phase). RNA purification was carried out as described previously (28). Primer extension analysis was performed using fluorescence-labeled probes according to the published procedure (27). In brief, 40 μg of total RNA and 1 pmol of 5′-FITC-labeled enhanced GFP primer with the sequence 5′-AGGGTCAGCTTGCCGTAGG-3′ were mixed in 20 μl of 10 mM Tris-HCl (pH 8.3 at 37°C); 50 mM KCl; 5 mM $MgCl_2$; 1 mM each of dATP, dTTP, dGTP, and dCTP; and 20 U of RNase inhibitor. The primer extension reaction was initiated by the addition of 5 U of avian myeloblastosis virus reverse transcriptase (Takara). After incubation for 1 h at 50°C, DNA was extracted with phenol, precipitated with ethanol, and subjected to electrophoresis on a 6% polyacrylamide sequencing gel containing 7 M urea. Fluorescence-labeled DNA in gels was detected using a slab gel DNA sequencer, DSQ-500L (Shimadzu).

Northern blotting analysis. Northern blot analysis of *nemR* and *nemA* RNAs was performed essentially as described previously (27). In brief, total RNAs were prepared by the hot phenol method from both *E. coli* wild-type KP7600 and *nemR*-disrupted mutant JD22799, separated by agarose gel electrophoresis in the presence of formamide, and transferred to a positively charged nylon membrane (Roche). The digoxigenin (DIG)-labeled probes were prepared with the PCR DIG probe synthesis kit (Roche) using a pair of oligonucleotides, nemR-F (5′-ATGGGGCTAAGCGAATTACTAAAAAC-3′) and nemR-R (5′-GCAAT AATGTTTTTTACATGGGCCAG-3′) for the 5′-proximal *nemR* probe or nemA-F (5′-GTACCGATCAGTACGGCGG-3′) and nemA-R (5′-TTACAAC GTCGGTGAATCGGTATAG-3′) for the 3′-proximal *nemA* probe. Hybridization was carried out at 50°C for 16 h in DIG Easy Hyb (Roche) as recommended by the supplier (Roche). The hybridized probe on a membrane was detected by CDP-Star, ready to use (Roche).

Quantitative immunoblot analysis. Antibodies against NemR were raised in rabbits by injecting them with the purified NemR protein. A quantitative Western blot analysis was carried out by standard methods as described previously (7). In brief, *E. coli* cells grown in 10 ml of either LB or M9-0.4% glucose medium were harvested by centrifugation and resuspended in 0.3 ml lysis buffer (50 mM Tris-HCl, pH 7.5, 50 mM NaCl, 5% glycerol, and 1 mM dithiothreitol), and then lysozyme was added to a final concentration of 20 μg/ml. Total proteins were subjected to 12% sodium dodecyl sulfate-PAGE and blotted onto polyvinylidene difluoride membranes using a semidry transfer apparatus. Membranes were first immunodetected with anti-NemR and then developed with an enhanced chemiluminescence kit (Amersham-Pharmacia Biotech). The image was analyzed with a LAS-1000 Plus Lumino-Image Analyzer and Image Gauge (Fuji Film).

RESULTS AND DISCUSSION

NemR, formerly named YdhM, is a member of the TetR family HTH-type DNA-binding transcription factor with a molecular mass of 22,275 Da consisting of 199 amino acid residues (18). However, neither gene targets of regulation nor regulatory mechanisms remain solved. From a series of experiments

TABLE 1. SELEX search for NemR-binding sites[a]

Left gene(s) (direction)	SELEX fragment (size; coding frame)	Right gene(s) (direction)	No. of fragments
ydhF-ydhL (←)	S (184–316 bp)	***nemR-nemA-gloA*** (→)	69
sapF-sapD-sapC-sapB (←)	S (200–257 bp; *sapA*)	*ymjA* (←)	14
leuE (←)	S (233–238 bp; *yeaT*)	***yeaU*** (→)	5
hslO (→)	S (184 bp; *yhgE*)	***pck*** (→)	3

[a] The genomic SELEX search for NemR-binding sequences was performed using purified His-tagged NemR alone in the absence of effectors. A total of 91 DNA fragments were isolated, of which 69 fragments contained sequences within spacer regions between *ydhL* and *nemR* coding frames. Three other kinds of SELEX fragments were located on *sapA*, *yeaT*, and *yhgE* coding frames. The arrows indicate the direction of transcription of the neighboring genes, and the genes shown in bold represent possible target genes under the control of NemR.

described in this report, we found that YdhM is the repressor for the *ydhM-nemA* operon, which encodes YdhM itself and NemA for NEM reductase. Thus, we propose to rename YdhM as NemR.

Screening of NemR-binding sequences by genomic SELEX. For the identification of DNA sequences that are recognized by *E. coli* NemR, we employed the genomic SELEX method (19), in which a complete library of *E. coli* genome DNA fragments is used instead of synthetic oligonucleotides with all possible sequences used in the original SELEX method (4, 23, 25). Into the mixture of *E. coli* genomic DNA fragments of 150 to 300 bp in length, a fourfold molar excess of the purified His-tagged NemR protein was added, and the NemR-DNA complexes were affinity purified. In the early stage of this genomic SELEX cycle, the NemR-bound DNA fragments gave smear bands on PAGE, as did the original genome fragment mixture. After two and three SELEX cycles, several discrete bands were identified, indicating that some DNA fragments with high affinity to NemR were enriched. These DNA fragments were recovered from the gel and cloned into pT7 Blue-T plasmid (Novagen) for sequencing.

A total of 91 clones were isolated from four regions (one spacer region and three different coding regions) of the *E. coli* genome (Table 1). Since regulatory proteins affecting transcription initiation generally bind upstream of their respective target genes, the regulation target of uncharacterized putative transcription factor NemR may be uncharacterized *ydhF-ydhL* and/or *nemR-nemA* (NEM reductase)-*gloA* (glyoxylase I), *sapABCDF* (peptide uptake ABC transporter), *leuE* (leucine export protein), *yeaU*, and *pck* (phosphoenolpyruvate carboxykinase).

Identification of NemR-binding DNA sequences. The binding of NemR protein to all four sequences identified by the SELEX screening was examined by gel shift assay. As shown in Fig. 1, all SELEX DNA fragments (*ydhL-nemR* spacer probe, *sapA* coding frame probe, *yeaT* coding frame probe, and *yhgE* coding frame probe) formed NemR complexes in a protein dose-dependent manner. The NemR binding to the *ydhL-nemR* spacer was observed at lower protein concentrations than was that to the other three target DNAs, and the NemR complex band with this *ydhL-nemR* probe was sharper than those with the other three probes. These observations indicate that the affinity of NemR is the highest for the *ydhL-nemR* spacer sequence, because the number of SELEX clone isolations correlates with the affinity of the test transcription factor for target DNA (15, 16, 19, 20).

To identify the recognition sequence of NemR binding, we next performed a DNase I footprinting assay using the *ydhL-nemR* SELEX fragment as a probe. After formation of complexes in the presence of a fixed amount of the fluorescence-labeled DNA probe and increasing amounts of NemR, DNase I treatment was carried out for a short period, and the partially digested DNA products were analyzed by PAGE (Fig. 2A). Clear protection by NemR was observed at a single region consisting of approximately 25 bp in length, in which a palindromic sequence, TAGACCnnnnGGTCTA, was included (Fig. 2B). Protection from DNase digestion by NemR was also observed for *sapA*, *yeaT*, and *yhgE* coding frame probes (data not shown), although the protection was not as clear as in the case of the *ydhL-nemR* probe.

Prediction for the NemR recognition sequence. After comparison of four DNase I-resistant sequences protected by NemR, we could identify a common 16-bp-long palindromic sequence, TAGACCnnnnGGTCTA, as the NemR recognition sequence, hereafter referred to as the NemR box (Fig. 2D). A total of 69 SELEX clones containing the *ydhL-nemR* spacer

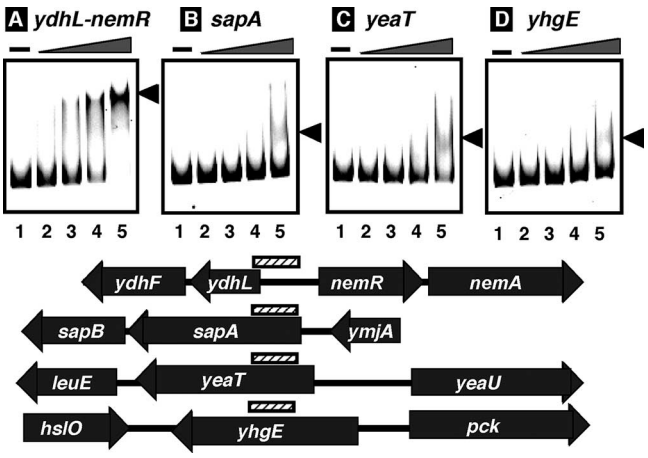

FIG. 1. Gel mobility shift assay of NemR-target DNA complex formation. Fluorescence-labeled DNA probes, 1.0 pmol each, containing a SELEX segment from the *ydhL-nemR* spacer (A), *sapA* coding frame (B), *yeaT* coding frame (C), and *yhgE* coding frame (D), were incubated at 37°C for 30 min in the absence (lanes 1) or presence of increasing concentrations of NemR (lanes 2, 0.25 pmol; lanes 3, 0.5 pmol; lanes 4, 1.0 pmol; lanes 5, 2.0 pmol). The reaction mixtures were directly subjected to PAGE. The gene organization and the location of probes along the *E. coli* genome are shown below the gel patterns. The functions of known genes are as follows: *nemA*, NEM reductase; *sapA*/*sapB*, antimicrobial peptide transporter subunits; *leuE*, neutral amino acid efflux system; *hslO*, heat shock protein Hsp33; *pck*, phosphoenolpyruvate carboxykinase.

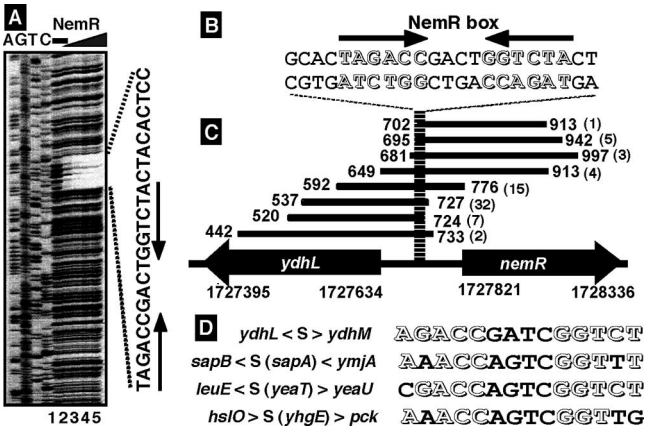

FIG. 2. Identification of the NemR box sequence. (A) DNase I footprinting of the NemR-binding site and the recognition sequences of NemR. The fluorescence-labeled SELEX segment (1.0 pmol) of the *ydhL-nemR* spacer region was incubated in the absence (lane 1) or presence of increasing concentrations of purified NemR (lane 2, 1.25 pmol; lane 3, 2.5 pmol; lane 4, 5.0 pmol; lane 5, 10 pmol) and then subjected to DNase I footprinting assays. Lanes A, T, G, and C represent the respective sequence ladders. (B) From the DNase I footprinting assay, a 22-bp-long sequence was found to be protected by NemR. (C) A total of 69 independent SELEX clones containing parts of the *ydhL-nemR* spacer sequence were aligned along the *E. coli* genome. The 22-bp sequence was present among all these 69 clones. The number of each SELEX clone is given in parentheses. (D) After alignment of four SELEX fragments, the consensus recognition sequence by NemR, designated the NemR box as shown on top of panel B, was predicted to be a palindromic sequence consisting of TAGAC CnnnnGGTCTA.

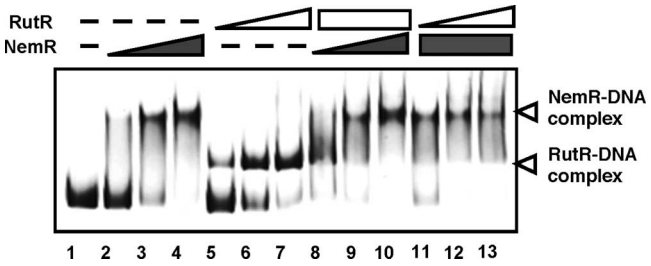

FIG. 3. Competition in DNA binding between NemR and RutR. Fluorescence-labeled *ydhL-nemR* spacer DNA probe (0.5 pmol; Fig. 2) was incubated at 37°C for 30 min in the absence (lane 1) or presence of increasing concentrations of NemR (lane 2, 0.5 pmol; lane 3, 1.0 pmol; lane 4, 2.0 pmol) or RutR (lane 5, 1.0 pmol: lane 6, 2.0 pmol; lane 7, 3.0 pmol). In the reactions shown in lanes 8 to 13, the increasing amounts of NemR (lane 8, 0.5 pmol; lane 9, 1.0 pmol; lane 10, 2.0 pmol) were added in the presence of a fixed amount of RutR (2.0 pmol) or the increasing amounts of RutR (lane 11, 1.0 pmol; lane 12, 2.0 pmol; lane 13, 3.0 pmol) were added in the presence of a fixed amount of NemR (2.0 pmol). The reaction mixtures were directly subjected to PAGE.

sequences included eight different fragments, ranging from 184 to 316 bp in length (Table 1). After alignment of all these eight different sequences, it turned out that a 22-bp overlapping sequence always existed in which the predicated 16-bp NemR box sequence was included (Fig. 2C). These findings altogether supported the prediction of a consensus 6 + 4 + 6 sequence consisting of TAGACCnnnnGGTCTA as the NemR box.

With use of this NemR box sequence, we searched for the location of the NemR box along the entire *E. coli* genome. The *ydhL-ydhM* spacer herein isolated was the only sequence that showed a complete match with the predicted NemR box (Table 1 and Fig. 2). Two sequences which contain one mismatch with the NemR box were identified, one on the *yeaT* coding frame (Table 1) and another on the *acrA* coding frame. A total of 32 sequences which contain two mismatches were identified. As discussed in the case of the RutR box, some of the sequences recognized by a test transcription factor may be lost after repeated SELEX cycles (20, 21).

Competition between NemR and RutR in binding to the NemR box. Interestingly the NemR box sequence TAGACC nnnnGGTCTA is close to the sequence recognized by RutR (RutR box), TTGACCAnnTGGTCAA. RutR is the uracil- and thymine-sensing master regulator of a set of genes for degradation and reutilization of pyrimidines (20). We then tested possible competition between RutR and NemR in binding to the *nemR* promoter. Even though the *nemR* promoter sequence was not included in the previous genomic SELEX by RutR (20), it turned out that in vitro screening was not saturated after chromatin immunoprecipitation chip analysis in vivo (21). As shown in Fig. 3, RutR indeed bound to the *nemR* promoter in a dose-dependent manner (Fig. 3, lanes 5 to 7). When increasing amounts of NemR were added in the presence of a high concentration of RutR that fully converted the fluorescence-labeled probe DNA forming RutR complexes, the probe was completely transferred from RutR complexes into NemR complexes (Fig. 3, lanes 8 to 10). On the other hand, increasing amounts of RutR were unable to replace the NemR-DNA complexes (Fig. 4, lanes 11 to 13). Taken together we concluded that the affinity of NemR for the *nemR* promoter, the common target between NemR and RutR, is higher than that of RutR. This finding suggests that the repression of the *nemR* promoter by RutR takes place only in the absence of NemR binding (or in a derepressed state).

Influence of NemR on in vivo promoter activity. The possible influence of NemR on transcription initiation from the *nemR* promoter within the *ydhL-nemR* spacer region was then examined using the two-fluorescent-protein promoter assay system. For this purpose, we first determined the location of the promoter within the SELEX fragment. Sequences of 488 bp, 483 bp, and 486 bp

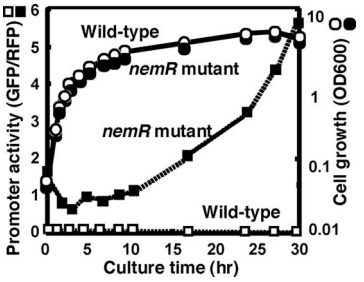

FIG. 4. Assay of the *nemRA* promoter in wild-type and *nemR* mutant *E. coli*. The *nemRA* operon promoter fragment was inserted into the two-fluorescent-protein promoter assay vector pGRP, and the resulting promoter plasmid was transformed into the KP7600 wild-type strain and its *nemR*-disrupted mutant JD22799. The promoter activity was determined by measuring the GFP/RFP ratio. The *nemRA* promoter activity was low in the wild type, but promoter activity was detected in the *nemR* mutant and increased after prolonged culture.

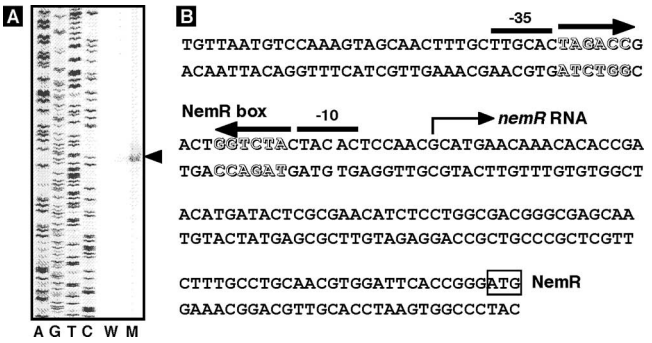

FIG. 5. (A) Primer extension analysis of *nemRA* mRNA. *E. coli* KP7600 (lane W) and *nemR* mutant JD22799 (lane M) were grown in LB medium. Total RNAs were prepared at late stationary phase and subjected to primer extension assays as described in Materials and Methods. The arrowhead indicates the transcription start site. (B) The transcription start site, shown by an arrow, is located 88 bp upstream from the initiation codon of the *nemR* gene. The NemR box is located between −13 and −28 from the *nemR* transcription initiation site.

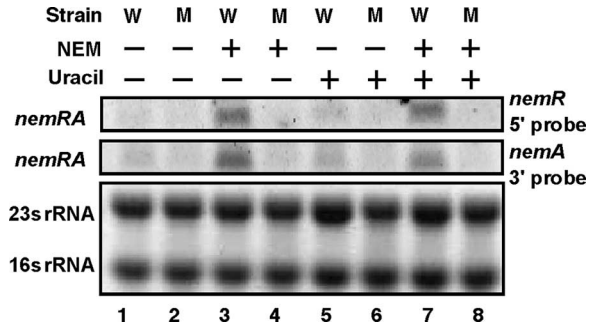

FIG. 6. Northern blot analysis of *nemRA* operon RNA. Overnight cultures of *E. coli* wild-type KP7600 (W) and its *nemR*-disrupted mutant JD22799 (M) in LB medium were transferred into fresh LB medium in the absence (lanes 1 and 2) or presence of 0.01 mM NEM (lanes 3 and 4), 0.1 mM uracil (lanes 5 and 6), or both NEM and uracil (lanes 7 and 8). Total RNA was isolated from each culture and fractionated by PAGE in the presence of urea. After RNA was blotted onto filters, *nemRA* RNA was detected with fluorescence-labeled *nemR* 5′ or *nemA* 3′ probe (upper panels) while rRNA was detected by ethidium bromide staining (lower panel).

upstream from the initiation codons of *ydhF*, *ydhL*, and *nemR* genes (Fig. 1 shows the gene organization) were inserted into pGRP vector to construct the promoter assay vectors pGRH043 (pGRP*ydhF*), pGRH044 (pGRP*ydhL*), and pGRH 045 (pGRP*nemR*), respectively. The expression of GFP is under the control of each test promoter, while RFP expression is directed by the reference promoter *lacUV5* on the same vector (see Materials and Methods). There should be a promoter for transcription toward *ydhLF*, but the expression of GFP was barely detected for the transformants with pGRH043 (*ydhF*) and pGRH044 (*ydhL*) vectors, implying that the promoters are very weak (in the case of *ydhL*) or absent (in the case of *ydhF*).

In contrast, the promoter activity was detected for the transformant with pGRH045 containing the *nemR* promoter sequence only when the transformant was grown in the *nemR* disruptant (Fig. 4). This finding suggests that NemR represses *nemA* expression under ordinary culture conditions. The *nemR* promoter-driven expression of GFP was detected not only in rich LB medium (Fig. 4) but also in poor M9-glucose medium even though the promoter activity was higher for cells grown in LB (data not shown). The *nemR* promoter activity increased after cells stopped growing, implying that the *nemR* promoter is one of the stationary-phase-specific promoters (9). Results of the promoter assay indicated that the *nemR* promoter is under the negative control of NemR for autogenous repression. Thus, we concluded that the NemR box is the operator for the NemR repressor.

Regulation in vivo of the *nemR* promoter by NemR. To confirm the above hypothesis, we directly determined the level of *nemR* mRNA in the presence and absence of NemR. To increase the sensitivity of detection, we isolated total RNAs from pGRH045 (pGRP*nemR*) transformants of both wild-type KP7600 and *nemR*-disrupted JD22799 and subjected them to primer extension analysis using the fluorescence (FITC)-labeled primer for detection of the 5′-proximal region of *nemR* mRNA (note that pGRH045 carries the *nemR* promoter sequence upstream from its initiation codon). As shown in Fig. 5A, a single initiation site of *nemR* transcription was identified at 88 bp upstream of the initiation codon for NemR synthesis. Since *nemR* mRNA was detected only in the *nemR*-disrupted mutant, we concluded that NemR is the repressor for transcription of its own gene. The NemR operator (NemR box) is located between −10 and −35 signals of the *nemR* promoter (Fig. 5B), implying that RNA polymerase binding to the *nemR* promoter interferes with NemR repressor.

Identification of *nemRA* transcription unit and effect of NEM on *nemRA* transcription. Since the promoter activity was not detected for the *nemR-nemA* spacer sequence (data not shown), we predicted that the *nemA* gene encoding NEM reductase forms a single operon with *nemR* and is cotranscribed from the *nemR* promoter. To examine this prediction, Northern blot analysis was performed using two different probes, the 5′-proximal sequence of *nemR* and the 3′-proximal sequence of *nemA*. A single RNA band of the expected size (approximately 1.8 kb) was detected using both probes at the same position (Fig. 6), indicating that *nemR* and *nemA* are indeed cotranscribed into one and the same transcription unit.

To identify the inducer(s) that inactivates NemR repressor for induction of the *nemRA* operon, growth was compared between the wild type and the *nemR* disruptant on the phenotype microarray (Biolog), but we failed to find compounds that affected growth differences between the two strains (data not shown). Since *nemR* forms a single operon with *nemA* encoding NEM reductase, we then examined the possible influence of NEM on the NemR activity. By addition of NEM to the wild-type culture, *nemRA* transcript significantly increased (Fig. 6, compare lanes 1 and 3), indicating that NEM is the inducer for derepression of the *nemRA* operon.

For disruption of the *nemR* gene in the mutant JD22799, a transposon was inserted into the *nemR* gene in opposite orientation from the NemR coding frame, thereby inhibiting *nemR* expression. In the mutant, transcription of the downstream *nemA* gene was also inhibited (Fig. 6, compare lanes 3 and 4), supporting the prediction that *nemR* and *nemA* form a single transcription unit and are cotranscribed into a single transcription unit.

RutR, the global regulator of the genes for synthesis and

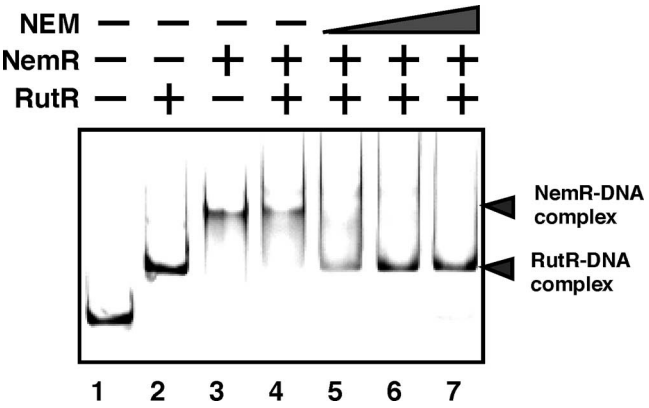

FIG. 7. Effect of NEM on DNA-binding activity of NemR. Fluorescence-labeled *ydhL-nemR* spacer DNA probe (0.2 pmol; Fig. 2 and 6) was incubated at 37°C for 30 min in the absence (lane 1) or presence of either NemR (lane 3, 1.0 pmol) or RutR (lane 2, 1.0 pmol). In the reaction shown in lane 4, fixed amounts of both NemR and RutR were added. In addition, increasing concentrations of NEM were added (lane 5, 0.1 nmol; lane 6, 1.0 nmol; lane 7, 10 nmol). The reaction mixtures were directly subjected to PAGE.

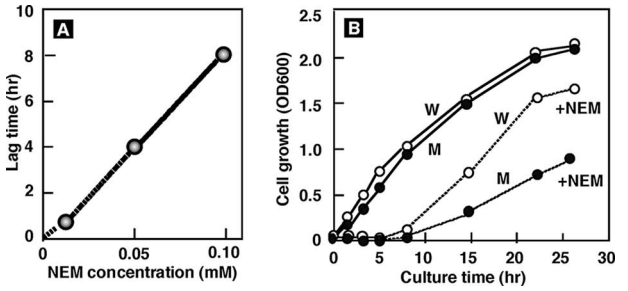

FIG. 8. Effect of NEM on cell growth. Overnight cultures of *E. coli* wild-type KP7600 (W) and its *nemR*-disrupted mutant JD22799 (M) in LB medium were transferred to fresh LB medium with or without 0.01, 0.05, and 0.10 mM NEM, and cell growth was monitored by measuring the turbidity at 600 nm. (A) Lag time before the entry into growth phase was plotted against NEM concentrations. (B) Growth curves of wild type (W) and mutant (M) in the absence (solid line) or presence (dashed line) of 0.10 mM NEM.

degradation of pyrimidines (19), binds to the same region as NemR does (Fig. 3). The possible influence of uracil on *nemRA* transcription was then examined by Northern blot analysis. No significant effect on the *nemRA* mRNA level was observed (Fig. 6, lanes 5 and 6). In the presence of both NEM and uracil, the induction of *nemRA* transcription was as high as that with NEM alone (Fig. 6, compare lanes 3 and 7). The induction of *nemRA* was not detected for the *nemR*-disrupted mutant (Fig. 6, compare lanes 1 and 2, lanes 3 and 4, lanes 5 and 6, and lanes 7 and 8). These results altogether further indicated that NEM is the inducer for derepression of *nemRA* transcription. Even though RutR binds to the NemR box (Fig. 3), RutR may not play an important role in regulation of *nemRA* expression in vivo.

Identification of NEM as an effector controlling NemR activity. The effect of NEM on the operator DNA-binding activity of NemR was then analyzed by gel shift assay. The binding in vitro of NemR to the *nemR* operator was completely disrupted by the addition of NEM (data not shown). To confirm this finding, we next performed a mixed gel shift assay, in which the binding of NemR and RutR to the same target, i.e., the *nemR* operator, was examined in the presence and absence of NEM. When both NemR and RutR were present, the NemR-*nemR* operator complex was preferentially formed, but after addition of NEM, the NemR-*nemR* operator complex disappeared and instead the RutR-*nemR* complex was formed (Fig. 7). These observations indicate that transcription of *nemA* must usually be repressed by NemR but is induced by the addition of NEM for degradation of NEM. Taking all these observations together, we predicted that the NemRA system plays an important role in *E. coli* survival in the presence of toxic NEM.

Inhibitory effect of NEM on cell growth and protective role of NemA expression. NEM is a specific reagent of Cys modification in proteins and a toxic compound for cell growth. The effect of NEM on *E. coli* growth was examined by following cell growth in the continuous presence of various concentrations of NEM. Above 0.01 mM NEM, the entry into exponential growth phase was significantly delayed, and the length of the lag period correlated with the NEM concentration (Fig. 8A). At 0.1 mM NEM, the entry into exponential growth phase was delayed for 8 h (Fig. 8B). This finding indicates that cell growth is initiated after expression of NEM reductase for effective degradation of toxic NEM. Accordingly, the higher level of NEM reductase may be needed for growth at higher concentrations of NEM.

Growth of this *nemR*-disrupted mutant was also examined in the presence of various concentrations of NEM. As expected from the *nemRA* single operon prediction (see above), the lag time was slightly elongated and, moreover, the rate of mutant cell growth after entry into growth phase was significantly lower than that of the wild-type parent (Fig. 8B). Thus, we concluded that NemA is essential for cell growth in the presence of NEM.

Activity control of NemR transcription factor by protein alkylation. NEM is a potent and specific reagent of Cys modification. The NemR protein contains five Cys residues in a total of 199 residues. If the binding of NEM to one or more Cys residues renders NemR inactive, Cys modification reagents other than NEM might induce *nemRA* transcription. Showdomycin, 3-β-D-ribofuranosyl-1*H*-pyrrole-2,5-dione, is an antineoplastic and bactericidal antibiotic isolated from *Streptomyces showdoensis* (3, 13). At the molecular level, showdomycin is a potent inhibitor of enzymes such as UMP kinase (PyrH) and uridine phosphorylase (Udp) involved in pyrimidine synthesis and is a potent sulfhydryl reagent (26). The addition of showdomycin indeed inactivated NemR as measured by gel shift assay (Fig. 9A, lane 4). Likewise iodoacetate (IA), a weak alkylating agent which acts on Cys residues in proteins and is often used to modify SH groups to prevent reformation of disulfide bonds after reduction of Cys residues, also rendered NemR inactive, albeit at a lower level, with respect to its binding to target DNA (Fig. 9A, lane 7) (note that unbound probe was detected in the case of IA). A slight reduction of NemR-operator DNA complexes was also observed with methylglyoxal (Fig. 9A, lane 8), which reacts with proteins, mainly at Lys and Arg residues, to form glycation products. However, other agents with protein modification did

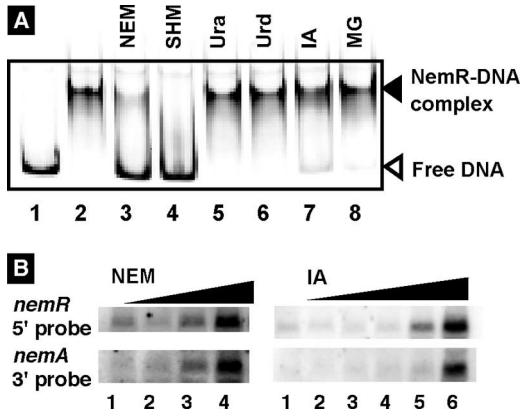

FIG. 9. Effect of Cys modification agents on NemR activity. (A) Effect on the in vitro DNA-binding activity of NemR. Fluorescence-labeled *ydhL-nemR* spacer DNA probe (Fig. 2, 6, and 7) was incubated at 37°C for 30 min with (lanes 2 to 8) or without (lane 1) NemR in the presence of 10 nmol each of NEM (lane 3), showdomycin (lane 4, SHM), uracil (lane 5, Ura), uridine (lane 6, Urd), IA (lane 7), or methylglyoxal (lane 8, MG). The reaction mixtures were directly subjected to PAGE. (B) Effect on the in vivo repressor activity of NemR. NEM or IA was added for 20 min to overnight LB culture of *E. coli* KP7600. RNA was prepared and subjected to Northern blot analysis using two types of DIG-labeled probe, *nemR* 5′ probe and *nemA* 3′ probe. The concentrations of NEM were 0, 1, 3, and 10 μM in lanes 1 to 4, respectively, while those of IA were 0, 1, 3, 10, 30, and 100 μM in lanes 1 to 6, respectively.

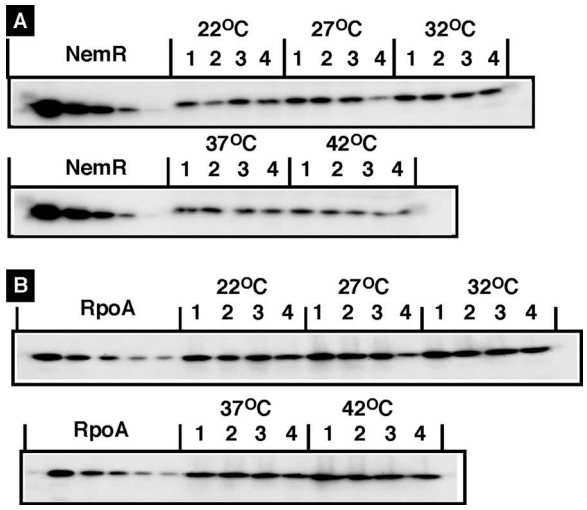

FIG. 10. Western blot analysis of whole-cell lysates with anti-NemR antiserum. Wild-type *E. coli* KP7600 was grown in LB and M9-0.4% glucose media at various temperatures from 20 to 42°C and for various times. At various growth phases (lanes 1 to 4, OD_{600}s of 0.3, 0.6, 0.9, and 1.5, respectively), whole-cell lysates were prepared and subjected to quantitative Western blot analysis against anti-NemR (A) and anti-RpoA (B) antibodies. The intensity of immunoblot bands was measured with a LAS-1000 Plus Lumino image analyzer and Image Gauge (Fuji Film).

not affect the DNA-binding activity of NemR, including succinimide, which forms covalent bonds with proteins (data not shown). Substrates for pyrimidine synthesis such as uracil (Fig. 9A, lane 5) and uridine (Fig. 9A, lane 6) did not affect NemR activity even though uracil is a potent inducer of RutR repressor for genes in the pathways for the synthesis and degradation of pyrimidine (20).

To examine the in vivo role of Cys modification agents other than NEM, Northern blot analysis was performed for RNA samples from wild-type *E. coli* cells in the presence of IA. In the presence of IA in LB culture medium, the growth of the *nemR* mutant was slightly retarded even though the effect was much weaker than that of NEM (data not shown). In the case of NEM, the induction of *nemRA* transcription was observed at concentrations as low as 3 μM (Fig. 9B, lane 3). In contrast, the induction of *nemRA* mRNA was observed in the presence of more than 30 μM IA (Fig. 9B).

Taking all the in vitro and in vivo observations together, we propose that the activity of NemR regulator is controlled by alkylation of one or more of its Cys residues. NemR contains five Cys residues at positions 70, 78, 88, 121, and 125 in a total of 199 residues. The critical Cys residue(s) involved in NemR activity control remains to be identified.

Intracellular level of NemR. A systematic measurement of the intracellular levels of a total of 150 transcription factors indicates that NemR is one of the more abundant transcription factors in *E. coli* W3110 (A. Ishihama, unpublished data), from which wild-type strain KP7600 originates. The intracellular concentration of NemR stays rather constant at a level close to that of RNA polymerase α subunit (about 5,000 molecules per genome equivalent of DNA) throughout growth phases from early log to stationary phase and at various temperatures from 22 to 42°C as determined by quantitative immunoblot analysis (Fig. 10). Thus, the level of functional NemR must be controlled by interconversion between effector-bound inactive and DNA-bound active forms. In the absence of inducers such as NEM, NemR must stay as an active repressor at least against the *nemRA* operon. Since NemR repressor is one of the more abundant transcription factors in *E. coli*, it may regulate target genes and promoters other than the *nemRA* operon. The possible involvement of NemR in regulation of other targets including *sapA*, *yeaT*, and *yhgE* (and genes located in their flanking sequences) remains to be examined. Upon exposure to external chemicals with protein alkylation activity, however, a set of target genes should be expressed. Taken together, we propose a novel mode of the activity control of NemR transcription factor by protein alkylation with external agents in the environment. It is noteworthy that the activity of transcription factors involved in regulation of the genes for detoxification of toxic environmental compounds is controlled by a set of chemicals present in nature.

Along this line, it is worthwhile to note that the *gloA* gene located downstream of the *nemA* gene is also involved in degradation of toxic compounds in the environment. The *gloA* gene encodes glyoxalase I (GlxI), the first enzyme in the ubiquitous glyoxalase system for conversion of toxic alpha-ketoaldehydes into their corresponding nontoxic 2-hydroxycarboxylic acids, utilizing glutathione as a cofactor (2, 8). GloA is also involved in potassium efflux through the KefB and KefC system because the product of glyoxalase I activity, *S*-lactoylglutathione, is the activator of KefBC (8). Glx enzymes are generally zinc-containing metalloenzymes, but *E. coli* GloA glyoxalase I contains nickel as a cofactor (2). Thus, both *nemA* and *gloA* are involved in degradation of toxic compounds for detoxification and reuse as nitrogen sources. At present, how-

ever, it is not known yet whether these two genes are organized into a single operon.

ACKNOWLEDGMENTS

We thank Takenori Miki (Fukuoka Dental College) for the *nemR*-disrupted mutant JD22799 and H. Ogasawara, J. Teramoto, and K. Yamamoto (Hosei University) for discussion.

This work was supported by grants-in-aid (17076016 and 18310133) from the Ministry of Education, Culture, Sports, Science and Technology of Japan and the Nano-Biology Project of the Micro-Nano Technology Research Center of Hosei University.

REFERENCES

1. **Ackerley, D. F., C. F. Gonzalez, M. Keyhan, R. Blake, and A. Martin.** 2004. Mechanism of chromate reduction by the *Escherichia coli* protein, NfsA, and the role of different chromate reductases in minimizing oxidative stress during chromate reduction. Environ. Microbiol. **6:**851–860.
2. **Clugston, S. L., J. F. Barnard, R. Kinach, D. Miedema, E. Daub, and J. F. Honek.** 1998. Overproduction and characterization of a dimeric non-zinc glyoxalase I from *Escherichia coli*: evidence for optimal activation by nickel ions. Biochemistry **37:**8754–8763.
3. **Darnall, K. R., L. B. Townsend, and R. K. Robins.** 1967. The structure of showdomycin, a novel carbon-linked nucleoside antibiotic related to uridine. Proc. Natl. Acad. Sci. USA **57:**548–553.
4. **Ellington, A. D., and J. W. Szostak.** 1990. *In vitro* selection of DNA molecules that bind specific ligands. Nature **346:**818–822.
5. **Gonzalez-Perez, M. M., P. van Dillewijin, R. M. Wittich, and J. L. Ramos.** 2007. *Escherichia coli* has multiple enzymes that attack TNT and release nitrogen for growth. Environ. Microbiol. **9:**1535–1540.
6. **Ishihama, A., and J. Hurwitz.** 1969. The role of deoxynucleic acid in ribonucleic acid synthesis. XVII. Multiple active sites of *Escherichia coli* ribonucleic acid polymerase. J. Biol. Chem. **255:**6680–6689l.
7. **Jishage, M., A. Iwata, S. Ueda, and A. Ishihama.** 1996. Regulation of RNA polymerase sigma subunit synthesis in *Escherichia coli*: intracellular levels of four species of sigma subunit under various growth conditions. J. Bacteriol. **178:**5447–5451.
8. **MacLean, M. J., L. S. Ness, G. P. Ferguson, and I. R. Booth.** 1998. The role of glyoxalase I in the detoxification of methyglyoxal and in the activation of the KefB K+ efflux system in *Escherichia coli*. Mol. Microbiol. **27:**563–571.
9. **Makinoshima, H., A. Nishimura, and A. Ishihama.** 2002. Fractionation of *Escherichia coli* cell populations at different stages during growth transition to stationary phase. Mol. Microbiol. **43:**269–279.
10. **Miura, K., Y. Tomioka, H. Suzuki, M. Yonezawa, T. Hishinuma, and M. Mizugaki.** 1997. Molecular cloning of the *nemA* gene encoding N-ethylmaleimide reductase from *Escherichia coli*. Biol. Pharm. Bull. **20:**110–112.
11. **Moore, P. B.** 1971. Reaction of N-ethylmaleimide with the ribosomes. J. Mol. Biol. **60:**169–184.
12. **Nakabeppu, Y., and M. Sekiguchi.** 1986. Regulatory mechanisms for induction of synthesis of repair enzymes in response to alkylating agents: ada protein acts as a transcriptional regulator. Proc. Natl. Acad. Sci. USA **83:** 6297–6301.
13. **Narayanan, C. S., and J. S. Krakow.** 1983. Chemical modification of the sigma subunit of the *E. coli* RNA polymerase. Nucleic Acids Res. **11:**2710–2716.
14. **Nishimura, H., M. Mayama, Y. Komatsu, H. Kato, N. Shimaoka, and Y. Tanaka.** 1964. Showdomycin, a new antibiotic from a *Streptomyces* sp. J. Antibiot. **17:**148–155.
15. **Ogasawara, H., A. Hasegawa, E. Kanda, T. Miki, K. Yamamoto, and A. Ishihama.** 2007. Genomic SELEX search for target promoters under the control of the PhoQP-RstB signal cascade. J. Bacteriol. **187:**4791–4799.
16. **Ogasawara, H., Y. Ishida, K. Yamada, K. Yamamoto, and A. Ishihama.** 2007. PdhR (pyruvate dehydrogenase complex regulator) controls the respiratory electron transport system in *Escherichia coli*. J. Bacteriol. **189:**5534–5541.
17. **Rau, J., and A. Stolz.** 2003. Oxygen-insensitive nitroreductases NfsA and NfsB of *Escherichia coli* function under anaerobic conditions as lawsone-dependent azo reductases. Appl. Environ. Microbiol. **69:**3448–3455.
18. **Riley, M., T. Abe, M. B. Arnaoud, M. K. B. Berlyn, F. R. Blattner, R. R. Chaudhuri, J. D. Glasner, T. Horiuchi, I. M. Keseler, T. Kosuge, H. Mori, N. T. Perna, G. Plunkett III, K. E. Rudd, M. H. Serres, G. H. Thomas, N. R. Thomson, D. Wishart, and B. L. Wanner.** 2006. *Escherichia coli* K-12: a cooperatively developed annotation snapshot-2005. Nucleic Acids Res. **34:** 1–9.
19. **Shimada, T., N. Fujita, M. Maeda, and A. Ishihama.** 2005. Systematic search for the Cra-binding promoters using genomic SELEX systems. Genes Cells **10:**907–918.
20. **Shimada, T., K. Hirao, A. Kori, K. Yamamoto, and A. Ishihama.** 2007. RutR is the uracil/thymine-sensing master regulator of a set of genes for synthesis and degradation of pyrimidines. Mol. Microbiol. **66:**744–779.
21. **Shimada, T., A. Ishihama, S. J. W. Busby, and D. C. Grainger.** 2008. The Escherichia coli RutR transcription factor binds at targets within genes as well as intergenic regions. Nucleic Acids Res. **36:**3950–3955.
22. **Shimada, T., H. Makinoshima, Y. Ogawa, T. Miki, M. Maeda, and A. Ishihama.** 2004. Classification and strength measurement of stationary-phase promoters by use of a newly developed promoter cloning vector. J. Bacteriol. **186:**7112–7122.
23. **Singer, B. S., T. Shtatland, D. Brown, and L. Gold.** 1997. Libraries for genomic SELEX. Nucleic Acids Res. **25:**781–786.
24. **Slobin, L. I.** 1971. Sulfhydryl groups of *Escherichia coli* ribosomes and ribosomal proteins. J. Mol. Biol. **61:**281–286.
25. **Tuerk, C., and L. Gold.** 1990. Systematic evolution of ligands by exponential enrichment: RNA ligands to bacteriophage T4 DNA polymerase. Science **249:**505–510.
26. **Watanabe, S.** 1970. Equimolecular reaction of showdomycin with thiols. J. Antibiot. **23:**313–314.
27. **Yamada, M., H. Izu, T. Nitta, K. Kurihara, and T. Sakurai.** 1998. High temperature, nonradioactive primer extension assay for determination of a transcription initiation site. BioTechniques **25:**72–75.
28. **Yamamoto, K., H. Ogasawara, N. Fujita, R. Ustumi, and A. Ishihama.** 2002. Novel mode of transcription regulation of divergently overlapping promoters by PhoP, the regulator of two-component system sensing external magnesium availability. Mol. Microbiol. **45:**423–438.
29. **Yin, H., T. K. Wood, and B. F. Smets.** 2005. Reductive transformation of TNT by *Escherichia coli*: pathway description. Appl. Microbiol. Biotechnol. **67:**397–404.